



Comparative study on the topical and transdermal delivery of diclofenac incorporated in nano-emulsions, nano-emulgels, and a colloidal suspension

Estelle-Vionè Louw¹ · Wilna Liebenberg¹ · Clarissa Willers¹ · Admire Dube² · Marique E. Aucamp² · Minja Gerber¹

Accepted: 19 November 2022 / Published online: 16 December 2022
© Controlled Release Society 2022

Abstract

Transdermal delivery of active pharmaceutical ingredients (APIs) can be challenging, since the skin possesses a rate-limiting barrier, which may be overcome when APIs possess certain ideal physicochemical properties. The lack thereof would require that APIs be included in drug delivery vehicles to enhance skin permeation. Hence, diclofenac was incorporated into various drug delivery vehicles (i.e., nano-emulsions, nano-emulgels, and a colloidal suspension containing drug-loaded nanoparticles) to investigate the transdermal delivery thereof, while nano-emulsions and nano-emulgels had varying concentrations of evening primrose oil (EPO). The aim of the study was to compare the topical and transdermal diclofenac delivery from the different types of vehicles and to investigate the influence the different EPO concentrations had on diclofenac delivery. After characterization, membrane release studies were performed (to determine whether the API was successfully released from the vehicle) followed by *in vitro* skin diffusion studies and tape stripping (to establish whether the vehicles assisted the API in reaching the target site (transdermal delivery)). Lastly, cytotoxicity studies were conducted via methyl thiazolyl tetrazolium (MTT) and neutral red (NR) assays on human keratinocyte (HaCaT) cells. Results showed minimal cytotoxic effects at concentrations equivalent to that which had permeated through the skin, while the membrane release and *in vitro* skin diffusion studies indicated that the nano-emulsions and the 10% EPO vehicles increased API release and diffusion when compared to the other vehicles. However, the colloidal suspension had the highest concentrations of API within the skin. Hence, all the vehicles were non-toxic and effectively delivered diclofenac through the transdermal route.

Keywords Colloidal suspension · Diclofenac · Evening primrose oil · Nano-emulgel · Nano-emulsion · Transdermal drug delivery

Introduction

Inflammation is crucial for health, as it initiates the healing process [1]. Inflammation aggravates pain sensation, and the mismanagement thereof can negatively affect an individual's quality of life [2]. Symptomatic treatment of these conditions is achievable by inhibiting the inflammatory process

[3, 4]. Non-steroidal anti-inflammatory drugs (NSAIDs) are the leading approach for the treatment of pain [5]. The anti-inflammatory effects of NSAIDs are due to the inhibition of prostaglandin by blocking the cyclooxygenase (COX)-2 enzymes [6]. Non-selective NSAIDs (nsNSAIDs) also bind to the COX-1 enzyme that is responsible for gastrointestinal protection [7]. Diclofenac is a nsNSAID with a fast onset and long duration of action. However, extended oral administration often leads to adverse gastrointestinal effects due to the inhibition of COX-1 enzymes [8], which stresses the need for an alternative route of drug delivery, such as the transdermal route, for the administration of NSAIDs [5].

The skin is the largest, most accessible organ of the human body [9], but drug delivery proves challenging due to the rate-limiting outermost layer (stratum corneum) that functions as a barrier [10–13]. To overcome the stratum

✉ Minja Gerber
Minja.Gerber@nwu.ac.za

¹ Centre of Excellence for Pharmaceutical Sciences (Pharmacem™), North-West University, Private Bag X6001, Potchefstroom 2520, South Africa

² School of Pharmacy, Faculty of Natural Sciences, University of the Western Cape, Private Bag X17, Bellville, Cape Town 7535, South Africa

corneum hindrance during transdermal drug delivery, active pharmaceutical ingredients (APIs) require certain ideal physicochemical properties [14], i.e., molecular weight (< 500 Da), aqueous solubility (> 1 mg/ml) [14], partition coefficient ($\log P$ between 1 and 3) [9, 15], pH (3–9) [14] and melting point (< 200 °C) [14, 16]. It became evident that diclofenac did not possess all these ideal physicochemical properties. Hence, penetration enhancers (i.e., evening primrose oil (EPO)) and/or the inclusion of the API into a drug delivery vehicle (i.e., nano-emulsions (NEs), nano-emulgels (NGs), and a colloidal suspension (CS) containing drug-loaded nanoparticles (NPs)) can be used to improve drug delivery transdermally [17].

NEs are dispersions of two immiscible phases (oil and water) that form droplets with sizes ranging between 20–500 nm [18]. The nanometric-sized droplets offer increased skin permeation and stability [19], while the hydrophilic and lipophilic characteristics, attained from the two phases, allow for numerous applications in drug delivery through the stratum corneum [20]. Oil-in-water (o/w) NEs are mainly used to deliver lipophilic APIs, such as diclofenac [21], and can subsequently be formulated by means of a high-energy emulsification method that allows for the formation of ultra-small/nanometric droplets [22].

NGs possess all the ideal properties associated with NEs, as they are formulated by adding a gelling agent to the aqueous phase of the optimized NEs [23], which increases the viscosity of the NEs to allow for easy topical application and extended contact time between the drug delivery vehicle and the surface of the skin [24–26]. Carbopol® Ultrez 20 is a fast absorbing and easy wetting gelling agent, well known for its increased reproducibility and enhanced stability over a large pH range [26, 27].

CS containing suspended drug-loaded NPs have gained significant interest in recent years due to its various uses in the field of nanotechnology [28]. NPs are synthesized by means of an emulsion-solvent evaporation technique that results in nanometric-sized particles (1–100 nm) with a large volume-to-surface area ratio that enhances API release [29]. Drug-loaded NPs have enhanced stability, improved skin permeation, and decreased adverse effects and, depending on the type of NP, can have high solubility for either lipophilic or hydrophilic (double emulsion method) APIs [29, 30]. To produce a CS, NPs are suspended into a continuous aqueous phase, which acts as a carrier to assist in the transdermal delivery of the drug-loaded NPs [28].

The aim of this study was to formulate different drug delivery vehicles (like NEs, NGs, and a CS including drug-loaded NPs) containing diclofenac, while the NEs and NGs comprised of different EPO concentrations (natural oil acting as a penetration enhancer) to assist with transdermal delivery of diclofenac by altering the skin's protective barrier [31]. The drug delivery vehicles containing diclofenac

were investigated and compared during membrane release, in vitro skin diffusion, and tape stripping studies. The in vitro cytotoxicity of the NE (presenting with the highest skin diffusion results), a placebo, and the NPs was determined by methyl thiazolyl tetrazolium (MTT) and neutral red (NR) assays using human keratinocytes (HaCaT).

Materials and methods

Materials

Diclofenac (2-[(2,6-dichlorophenyl)amino]phenyl]acetic acid) (LEAPChem, HangZhou, CN) had a purity of 99.97%. Associated Chemical Enterprises (ACE) (Johannesburg, SA) provided analytical grade formic acid, chromatography grade acetonitrile, and methanol. A Direct Pure® Ultrapure laboratory water purification system (Merck-Millipore, Midrand, SA) supplied ultrapure water throughout the study. Formulation and phosphate buffer solution (PBS) excipients (sodium hydroxide (NaOH), potassium dihydrogen phosphate (KH₂PO₄), Span® 60 (lipophilic surfactant), Tween® 80 (hydrophilic surfactant), Carbopol® Ultrez 20, polycaprolactone (PCL), polyvinyl alcohol (PVA) and sucrose) came from Sigma-Aldrich (Johannesburg, SA), who also supplied dimethyl sulfoxide (DMSO), MTT, NR solution, non-essential amino acids (NEAA), and Triton™ X-100 for the cytotoxicity studies. CJP Chemicals (Johannesburg, South Africa) provided EPO, while LabChem (Johannesburg, SA) supplied the dichloromethane (DCM). Vertical Franz diffusion cells (2 ml) were sourced from PermeGear (Hellertown, PA, USA). Whatman® filter paper, Parafilm®, Dulbecco's Modified Eagle's Medium (DMEM) with high glucose (HyClone), and Dow Corning® high vacuum grease were procured from Separations (Randburg, SA). L-glutamine (200 mM), Trypan blue solution (0.4%), penicillin/streptomycin (pen/strep) (10,000 U/ml each), non-essential amino acids (NEAAs), and Trypsin-Versene® (EDTA) were purchased from Whitehead Scientific (Pty) Ltd. (Cape Town, South Africa). Fetal bovine serum (FBS) was acquired from Thermo Fisher Scientific (Gibco™, Johannesburg, South Africa).

Quantification of diclofenac

A Shimadzu® Nexera-i LC-2040C 3D Plus analytical instrument consisting of a quaternary pump, a wavelength detector, and an autosampler validated the analytical high-performance liquid chromatography (HPLC) method. The HPLC was operated with LabSolutions CDS software and fitted with a Venusil® XBP C₁₈(2), 2.1 × 150 mm; 5 μm; 100 Å column (Agela Technologies, Newark, DE). The isocratic system utilized 50% of both mobile phases, which consisted of (A) ultrapure water and 1.0% (v/v) formic acid and (B) chromatography grade acetonitrile with 0.1% (v/v) formic acid. A flow

rate of 1.0 ml/min was maintained throughout the analysis, with wavelengths detected at 230 nm. The total run time was set to 6.0 min, as diclofenac had a retention time of ± 5.4 min. The limit of detection (LOD) and limit of quantification (LOQ) of diclofenac were determined as 0.33 and 0.99 $\mu\text{g/ml}$, respectively. Before each experiment, a linear regression curve was obtained to quantify diclofenac.

Physicochemical properties of diclofenac

Solubility of diclofenac in PBS

Four test tubes were filled with 5 ml PBS (pH 7.4); three had an oversaturation of diclofenac, and the remaining test tube was a control (no API). The test tubes were left to stir for 24 h in a Grant[®] JB series water bath (Grant Industries, UK) fitted with a Variomag[®] magnetic stirring plate (Variomag, USA) and preheated to ~ 32 °C (temperature on the surface of human skin) [32]. Thereafter, the solutions were centrifuged at 11,000 rpm for 15 min. A 0.45- μm polytetrafluoroethylene (PTFE) filter was used to filter 1 ml of the supernatant into HPLC vials, and each analysis was done in duplicate.

Solubility of diclofenac in *n*-octanol

The solubility of diclofenac in *n*-octanol was determined with the same method stated in “[Solubility of diclofenac in PBS](#)”; however, the test tubes were filled with 5 ml *n*-octanol instead of PBS (pH 7.4). The supernatant (1 ml) was diluted with methanol (24 ml), filtered, and analyzed with HPLC.

Log D determination of diclofenac

Establishing the *n*-octanol solubility of diclofenac occurred prior to the log D (octanol–water distribution coefficient) determination thereof. The PBS (pH 7.4) and *n*-octanol were co-saturated by transferring equal amounts into a separating funnel, which was left to equilibrate for 24 h, forming two layers (bottom: PBS (pH 7.4) and top: *n*-octanol). After separating the two layers, pre-saturated *n*-octanol (20 ml) was used to dissolve the diclofenac (229 mg), in accordance with the solubility determined in “[Solubility of diclofenac in PBS and *n*-octanol](#)”. Three test tubes were filled with diclofenac/*n*-octanol solution (3 ml) and pre-saturated PBS (3 ml) and placed in a preheated (~ 32 °C) shaker water bath for 8 h, whereafter the test tubes were removed and left to equilibrate for 2 h. PBS (1 ml) from each test tube was extracted and filtered into HPLC vials. The diclofenac/*n*-octanol solutions (1 ml) were diluted with methanol (9 ml), filtered into HPLC vials, and analyzed. Lastly, a logarithmic ratio of the concentration of diclofenac detected in both the *n*-octanol and PBS (pH 7.4) phases established the log D of diclofenac.

Formulation of drug delivery vehicles

Different drug delivery vehicles containing diclofenac were formulated for transdermal delivery investigation. These drug delivery vehicles included NEs, NGs, and a CS containing drug-loaded NPs. Different concentrations of EPO were used during the formulation of the NEs and the NGs to establish whether the EPO concentration had an influence on drug delivery, which included an optimized NE-containing diclofenac and 10% EPO (NE10), 15% EPO (NE15), and 20% EPO (NE20). The placebos of NE10, NE15, and NE20 were NE10P, NE15P, and NE20P, respectively. The three NGs included an optimized NG containing diclofenac and 10% EPO (NG10), 15% EPO (NG15), and 20% EPO (NG20). Table 1 lists the composition of each drug delivery vehicle (CS (containing the NPs), NE10, NE15, NE20, NG10, NG15, and NG20).

Formulation of NEs containing diclofenac

The NEs were formulated at different EPO concentrations of 10, 15, and 20% (w/w) with a method adapted from Mduduzi et al. [33]. Diclofenac was added to EPO (oil phase) and stirred on a magnetic hot plate at ~ 90 °C until fully dissolved, after which Span[®] 60 was added. Tween[®] 80 was added to ultrapure water (water phase) and stirred on a magnetic hot plate at ~ 90 °C. Once the surfactants had fully dissolved, the oil phase was added dropwise into the continuously stirred water phase. This formed a coarse emulsion, which was left to stir for an additional 5 min. Thereafter, the coarse emulsion was placed in an ice bath and ultrasonicated for 6 min to form the NE [33].

Formulation of NGs containing diclofenac

The formulas of the optimized NEs were used to formulate the three NGs. The preparation of the oil phase was identical to that of the NEs (see “[Formulation of NEs containing diclofenac](#)” section). A concentration of 0.40% v/v of Carbopol[®] Ultrez 20 was added to the water phase after the dissolution of Tween[®] 80 in the ultrapure water. The water phase was sonicated for 1 min to remove any entrapped air bubbles and clamped to an overhead stirrer, and the oil phase was added in a dropwise manner, while stirring the mixture for 15 min to produce a coarse emulgel. The coarse emulgel was ultrasonicated for 3 min to form a NG [33]. The pH of the NGs were adjusted with NaOH (similar to the pH values of their respective NEs).

Formulation of a CS containing diclofenac-loaded NPs

An emulsion-solvent evaporation technique was used to synthesize the diclofenac-loaded NPs and required an organic and aqueous phase. The preparation of the aqueous phase involved

Table 1 Composition of the different drug delivery vehicles

Phase	Excipients	Drug delivery vehicle (% w/v)								
		NE10	NE15	NE20	NG10	NG15	NG20	NPs	CS	
Oil	Diclofenac	1.30	1.30	1.30	1.30	1.30	1.30	0.075*	–	
	Evening primrose oil	10.00	15.00	20.00	10.00	15.00	20.00	–	–	
	Span® 60	6.52	8.40	7.50	6.52	8.40	7.50	–	–	
Organic	PCL	–	–	–	–	–	–	0.025	–	
	DCM	–	–	–	–	–	–	24.90	–	
Solid	Diclofenac-loaded NPs	–	–	–	–	–	–	–	4.38*	
Aqueous	Ultrapure water	80.00	73.20	66.20	80.00	73.20	66.20	74.625	–	
	Tween® 80	2.17	2.10	5.00	2.17	2.10	5.00	–	–	
	Carbopol® Ultrez 20	–	–	–	0.40	0.40	0.40	–	–	
	PVA	–	–	–	–	–	–	0.375	–	
	PBS (pH 7.4)	–	–	–	–	–	–	–	95.62	

CS colloidal suspension, NE nano-emulsion, NG nano-emulgel, NP nanoparticle

*Instead of an oil phase, the NP has an organic phase, while the CS has a solid phase; diclofenac was included in these phases

dissolving PVA in ultrapure water and agitating the mixture on a magnetic hot plate at ~60 °C. To produce the organic phase, 0.075% w/v of diclofenac and 0.025% w/v of PCL were dissolved in 24.90% v/v of DCM. While the aqueous phase was sonicated, the organic phase was added dropwise with a syringe. The solution was sonicated for 12 min to form a milky solution. A rotary evaporator (Rotavapor® Büchi RII) was used to evaporate the DCM over a period of 20 min. Thereafter, the dispersion was centrifuged at 11,000 rpm for 30 min, and the supernatant was removed, leading to the formation of a pellet. Ultrapure water was added to the remaining pellet and placed in an ultrasonic bath for 15 min to re-disperse the pellet. Cryoprotectant (10 mg/ml sucrose solution) was added in a 1:2 ratio (protectant:ultrapure water), and the dispersion was placed in a –80 °C freezer for 12 h, followed by freeze-drying for 72 h. The NPs were placed in a desiccator for 72 h to remove excess moisture, prior to their suspension in PBS (pH 7.4) and subsequent diclofenac quantification with HPLC [34, 35].

Characterization of the drug delivery vehicles

The visual appearance, pH, droplet/particle size, polydispersity index (PDI), and the zeta-potential of all the drug delivery vehicles were investigated. Other characteristics were exclusively determined on certain drug delivery vehicles, such as viscosity (NEs and NGs) and morphology (NEs and dry NPs). X-ray powder diffraction analysis (XRPD) was conducted on the dry NPs.

Visual inspection

The formulated drug delivery vehicles underwent visual inspection for possible signs of flocculation, sedimentation, or aggregation.

pH

The pH measurements of the drug delivery vehicles were performed in triplicate by inserting a Mettler Toledo® InLab® 410 electrode into the drug delivery vehicle and recording the pH values displayed. The Mettler Toledo® pH meter (Mettler Toledo, CU) was calibrated beforehand at pH values of 4, 7, and 10 [33].

Droplet/particle size and PDI

Droplet/particle size and PDI measurements were done by means of a Malvern Zetasizer Nano ZS (Malvern Instruments, Worcestershire, UK) at a temperature of ~25 °C. Only a droplet of each NE and NG was transferred to a 100-ml volumetric flask and made up to volume with ultrapure water. The CS was ultrasonicated beforehand to disperse the particles. Clear disposable polystyrene cuvettes were filled with 2 ml of each dispersed solution and analyzed in triplicate [33, 35].

Zeta-potential

The same method and equipment described in “Droplet/particle size and PDI”, were used to determine the zeta-potential of the drug delivery vehicles in triplicate. However, 2 ml of each of the dispersed solutions were transferred into clear disposable capillary zeta-cells [33, 35].

Viscosity

The NEs and NGs were placed in a preheated water bath (~25 °C) an hour before measuring their viscosity. A Brookfield viscometer DV2T LV Ultra (Middleboro,

Massachusetts, USA) fitted with a TB-92 and a TF-96 spindle for the NEs and NGs, respectively, was used to measure the viscosity. Each preheated drug delivery vehicle was placed on the sample stand, and the Rheocalc T1.2.19 software was used to set the spindle rotation speed to 160 rpm and 100 rpm for the NEs and NGs, respectively. Multipoint data readings at 30-s intervals were performed over a period of 3 min and expressed in centipoise (cP) [33].

Morphology

The NEs were investigated by means of a transmission electron microscope (TEM) that utilized a FEI Tecnai G2 20S-Twin 200 kV HRTEM (Czech Republic, EU), equipped with an Oxford INCA X-Sight EDS System. During sample preparation, each NE (1 ml) was diluted with ultrapure water (49 ml). A small volume of the dilution was transferred onto a microscopic carbon-coated 300 mesh copper grid and left to dry whereafter, it was stained with osmium tetroxide and examined at ± 200 kV on the TEM. A Gatan bottom mount camera captured the micrographs, which were used to investigate the structural form of the NEs [33].

The dry NPs were investigated by means of a scanning electron microscope (SEM). The formulated dry NPs were attached to a small carbon tape that was mounted to a metal stub and coated with a gold–palladium film. Visualization of the NPs was done using a FEI Quanta 200 FEG SEM, with a 10 kV-accelerated voltage. The X-Max 20 EDS system (FEI, USA) captured the micrographs to investigate the surface texture, smoothness, and shape of the NPs [35].

XRPD analysis

XRPD identified the crystalline molecules or amorphous forms in the NPs and the compounds used during formulation. A PANalytical Empyrean diffractometer (PANalytical, Almelo, Netherlands) was used under the following measurement conditions: target, Cu; voltage, 40 kV; current, 30 mA; divergent slit, 2.0 mm; anti-scatter slit, 0.6 mm; detector slit, 0.2 mm; and monochromator scanning speed, 2°/min (step size, 0.025°; step time, 1.0 s). The samples (diclofenac, PCL, PVA, sucrose, and the formulated NPs) were spread evenly onto the zero-background sample holder and analyzed.

Skin experiments

Membrane release, followed by in vitro skin diffusion and tape stripping, was used to investigate the release, transdermal, and topical drug delivery of the formulated drug delivery vehicles, respectively each containing 1.3% (w/w) diclofenac. Prior to each diffusion study, the drug delivery

vehicle and its placebo were freshly formulated. PBS (pH 7.4) and the drug delivery vehicles were placed in separate water baths, preheated to ~ 37 °C (temperature of blood) or ~ 32 °C (temperature of the skin's surface), respectively, to ensure close replication of in vivo conditions. A total of 12 vertical Franz cells, each consisting of a donor and receptor chamber, were used: 10 cells for the drug delivery vehicles and two cells for the placebos.

Membrane release

A magnetic stirring rod was placed in the receptor compartment, while the donor and receptor compartments of the Franz cells were divided with polyvinylidene fluoride (PVDF; 0.45 μm) membranes. Vacuum grease was applied to the Franz cells, before being assembled and fastened with a horseshoe clamp to prevent any leakage. The receptor compartment was filled with 2 ml of PBS (pH 7.4), while ensuring no air bubbles formed. The Franz cells were placed in a preheated water bath (~ 37 °C) fitted with a magnetic stirring plate (Variomag, USA). The donor compartments received 1 ml of the respective drug delivery vehicle and were covered with a piece of Parafilm® to prevent moisture evaporation. Extraction and refilling of the receptor compartments with PBS (pH 7.4) occurred at hourly intervals for 6 h, followed by HPLC analysis of each extracted sample [33].

Skin preparation

Female Caucasian skin obtained after abdominoplasty was used during the skin studies. Skin donors gave informed consent before the skin was attained. Ethical approval from the North-West University Health Research Ethics Committee (NWU-HREC) was granted (ethics no.: NWU-00111–17-A1-10) prior to commencing with experiments.

The skin was inspected for any abnormalities that could affect the results of this study. Dermatomed skin (400 μm in width) was attained using a Zimmer™ electric dermatome (Zimmer 201 TDS, UK), placed on Whatman® filter paper, wrapped in aluminum foil, and stored at -20 °C. The skin was thawed on requirement, cut into circular pieces, and used during the skin diffusion studies [33].

In vitro skin diffusion

The Franz cells were prepared as explained in “[Membrane release](#)” except for the use of dermatomed skin (with the stratum corneum facing toward the donor phase) instead of membranes. After a pilot study was conducted, it was

observed that no diclofenac was detected in the first 20 min (0.33 h) after the extraction; hence, the extraction and refilling of the receptor phase occurred every 20 min, starting at 0.67 h up to 2 h, followed by two hourly intervals up until 12 h. Analysis occurred after transferring the extracted samples into HPLC vials [33].

Tape stripping

Tape stripping determined the amount of API that remained within the stratum corneum-epidermis (SCE) and epidermis-dermis (ED) after each skin diffusion study. The skin was dabbed with a paper towel to remove any remaining drug delivery vehicle. A strip of 3 M Scotch® Magic™ tape was cut into 12 pieces (± 2 cm). Each tape was pressed onto the diffused area of the skin and immediately removed. After discarding the first piece to avoid possible contamination, the remaining 11 pieces of tape containing the API and SCE went into a polytop-containing methanol (5 ml). After cutting the diffusion area of the residual skin sample (ED) into small pieces, it was placed in a separate polytop filled with methanol (5 ml); this was repeated for all 12 Franz cells, whereafter the polytops were stored in a refrigerator at ~ 4 °C for ± 8 h. Subsequently, the samples were filtered into HPLC vials and analyzed [33].

Data analysis for skin experiments

Samples from the membrane release, in vitro skin diffusion, and tape stripping studies were analyzed by HPLC after a linear regression curve was obtained to quantify the diclofenac concentration in the samples. For the membrane release and in vitro skin diffusion studies, the cumulative amount of diclofenac per area released and diffused ($\mu\text{g}/\text{cm}^2$), respectively were plotted against time (h), and the slope of the linear regression curve represented the flux ($\mu\text{g}/\text{cm}^2 \text{ h}$). The average and median flux values were determined for both the membrane release and in vitro skin diffusion studies. During the membrane release studies, the steady-state flux for each drug delivery vehicle was from 3 to 6 h. Furthermore, during the in vitro skin diffusion studies, it was observed that there was a consistent flow at two varying time intervals; consequently, two steady-state fluxes were obtained for each drug delivery vehicle, namely flux 1 from 0.67 to 2.00 h and flux 2 from 6.00 to 12.00 h. The average % released from the drug delivery vehicles was also determined [33].

For the analysis of the topical data (tape stripping), the average and median concentration ($\mu\text{g}/\text{ml}$) of diclofenac that permeated the SCE and the ED from the drug delivery vehicles were determined [33].

Cytotoxicity experiments

Cell-culturing conditions

The HaCaT cells were donated by Prof. Joana Miranda from the Department of Toxicological and Bromatological Sciences, Faculty of Pharmacy, University of Lisbon, Portugal. DMEM enhanced with 1% pen/strep (10,000 U/ml each), 1% NEAAs, 2 mM L-glutamine, and 10% FBS was used for the culturing and maintenance of the HaCaT cells. An ESCO CelCulture CO₂ incubator (Esco Technologies, Inc., USA) at ~ 37 °C, 5% CO₂, and 95% humidity was used for the incubation of the cells. Every 48 h, the cells were visually inspected under an inverted light microscope for confluency estimation and unwanted contamination, whereafter the culture medium was replaced. Sub-culturing occurred at ~ 80 – 90% confluency by measuring the concentration of viable cells in the cell suspension with trypsinization (EDTA and a 0.4% Trypan blue exclusion method) [36]. A seeding solution with a concentration of 75,000 cells/ml was prepared, of which 200 μl was transferred into each well of a 96-well plate to obtain a density of 15,000 cells/well, as required for the cytotoxicity assays. The seeded well plates were incubated for 24 h to allow cell recovery before initiating treatment.

Once the cells were recovered, they were exposed to the various treatment solutions for 12 h. The treatment concentrations were as follows: diclofenac solution (6.25–125.00 $\mu\text{g}/\text{ml}$), NE10 (6.50–130.00 $\mu\text{g}/\text{ml}$), NE10P (6.50–130.00 $\mu\text{g}/\text{ml}$), and NPs (1.25–25.00 $\mu\text{g}/\text{ml}$). Cytotoxicity studies were only performed on the NE with the highest diffusion results, the placebo thereof, and the NPs. The NE and its placebo were dissolved in methanol, followed by culture medium to obtain the desired treatment concentrations and to ensure that the methanol concentration that the cells were exposed to never exceeded 5%. The NPs were firstly diluted in phosphate-buffered saline and then in culture medium.

MTT assay

The MTT assay was done according to the method published by Fouché et al. [37]. After 12 h exposure, the treatment was extracted, the cells were washed in duplicate with 100 μl phosphate-buffered saline, and 200 μl of MTT solution (0.5 mg/ml in non-supplemented DMEM) was added to each well. The plate was covered with aluminum foil and incubated for 4 h at ~ 37 °C, 5% CO₂, and 95% humidity. Thereafter, the MTT solution was removed, and 200 μl DMSO was added to each well. The plate was placed on an orbital shaker for 1 h, followed by the measurement of absorbance at 560 and 630 nm with a SpectraMax® Paradigm® multi-mode microplate reader (Molecular

Devices, CA, USA). Additionally, the three control groups were included on the well plates: an untreated group (cells left untreated), a DMSO blank, and a dead cell group (10–15 min treatment of cells with phosphate-buffered saline containing 0.2% Triton™ X-100).

NR assay

The method published by Wentzel et al. [38] was modified for the purpose of the NR assay. Extraction and rinsing of the cells were done as stated in “MTT assay” whereafter 200 µl of NR solution (0.033% in non-supplemented DMEM, filtered through a 0.45 µm syringe filter) was added to each well. The plates were wrapped in aluminum foil and incubated for 2 h at ~37 °C, 5% CO₂, and 95% humidity, followed by the addition and immediate extraction of 100 µl of fixative (1% calcium chloride in 0.5% formaldehyde). Lastly, 150 µl NR-solubilization solution (1% acetic acid in 50% ethanol) was added and left on the orbital shaker for 10 min after covering the plate. Using the same microplate reader as for the MTT assay, the absorbance was measured at 540 and 690 nm. A solubilization blank was added instead of the DMSO group, while the other control groups remained the same.

Calculation of the IC₅₀ values

The in vitro cytotoxicity results were used to calculate the half-maximum inhibitory concentration (IC₅₀ value) of each treatment group. The assays were performed in two independent experiments, and each plate contained three wells with the same treatment concentration (hence, investigated six times per treatment group). The following equation was utilized to calculate the %cell viability [37]:

$$\% \text{Cell viability} = \frac{(\Delta \text{ Sample} - \Delta \text{ blank})}{(\Delta \text{ Untreated control} - \Delta \text{ blank})} \times 100 \quad (1)$$

where Δ represents the difference between measured absorbance values with the MTT (560–630 nm) or NR (540–690 nm) assays. The calculated %cell viability was subtracted from 100% to determine the %cell inhibition. The calculation of the IC₅₀ value (x -value) was done by means of a linear regression curve, where (y) represents the cell viability, (m) the slope of the curve, and (c) the y -intercept [39].

Statistical data analysis

Interferential statistical data analysis was conducted by using STATISTICA® 13.3 (StatSoft, TIBCO® Software Inc., USA) software.

One-way analysis of variance (ANOVA) was done on the diffusion data, whereas two-way ANOVA was performed on the tape stripping data. The data violated the assumptions of ANOVA, and consequently, log transformations were required as remedial [40]. An ANOVA omnibus F -test, followed by a Bonferroni adjustment, was done for multiple comparisons between the different drug delivery vehicles. A p -value of < 0.05 was considered statistically significant [41].

Results and discussion

Physicochemical properties of diclofenac

Solubility of diclofenac in PBS and *n*-octanol

An API is required to have an aqueous solubility above 1 mg/ml for transdermal drug delivery [14]; however, the experimentally calculated solubility of diclofenac in PBS (pH 7.4) was 0.913 ± 2.044 mg/ml. Although the solubility in PBS (pH 7.4) is close to the required value, diclofenac might have difficulty diffusing through the skin due to its low aqueous solubility. The solubility of diclofenac in *n*-octanol was determined as 11.451 ± 0.412 mg/ml, which may indicate that diclofenac might prefer to stay in the lipophilic SCE. Despite all this, PBS (pH 7.4) should suffice as receptor medium during the membrane release and skin diffusion studies, as it is recommended that lipophilic compounds, such as diclofenac, must partition freely into the receptor phase during diffusion studies [42]. Therefore, no other excipients or solubilizers were included with PBS (pH 7.4) in the receptor fluid of the Franz diffusion cells.

Log D of diclofenac

A log D higher than -1 indicates a lipophilic nature, contrary to a hydrophilic nature indicated by a log D lower than -1 [40, 43]. An API should possess both lipophilic and hydrophilic characteristics with a log D between 1 and 3 to ideally permeate through the skin [9]. The log D of diclofenac was calculated as 1.365 ± 0.003 , indicating that diclofenac is a more lipophilic in nature (higher than -1), and it might be ideal for transdermal diffusion (log D between 1 and 3) [11, 40, 43].

Characterization of the drug delivery systems

Table 2 summarizes the characterization results of the drug delivery vehicles. Figure 1 displays the visual appearance of the formulations, Fig. 2 displays the TEM and

Table 2 Characterization results obtained for each drug delivery vehicle

Drug delivery vehicle	pH	Droplet/particle size (nm)	PDI	Zeta-potential (mV)	Viscosity (cP)
NE10	5.925 ± 0.048	108.40 ± 3.020	0.246 ± 0.042	-35.9 ± 2.85	31.17 ± 0.19
NE15	6.145 ± 0.003	88.61 ± 1.750	0.247 ± 0.019	-33.3 ± 0.55	38.63 ± 0.20
NE20	5.518 ± 0.008	85.07 ± 1.102	0.175 ± 0.029	-36.6 ± 2.68	37.69 ± 0.26
NG10	5.940 ± 0.040	113.40 ± 2.130	0.261 ± 0.035	-41.1 ± 3.72	7,650.00 ± 115.67
NG15	6.054 ± 0.009	93.20 ± 0.967	0.420 ± 0.028	-53.1 ± 0.90	5,750.80 ± 211.30
NG20	5.671 ± 0.020	93.21 ± 1.847	0.472 ± 0.087	-31.7 ± 1.55	3,950.80 ± 19.46
CS	7.048 ± 0.010	225.10 ± 1.200	0.318 ± 0.067	-7.3 ± 0.42	-

CS colloidal suspension, *NE* nano-emulsion, *NG* nano-emulgel

SEM micrographs for the NEs and NPs, and Fig. 3 displays the XRPD results.

Each drug delivery vehicle underwent visual inspection after formulation (Fig. 1). The NEs had a white, milky liquid with no signs of aggregation, sedimentation, or any oil droplets. The NGs visibly portrayed a higher viscosity with a smooth, gel-like appearance and no signs of flocculation, sedimentation, or aggregation of droplets. The CS had a slightly white watery appearance and showed signs of sedimentation after ± 1 h (which may be due to oversaturation).

Transdermal drug delivery vehicles are required to have a pH value between 3 and 9 to prevent skin irritation [44]; hence, all the drug delivery vehicles displayed pH values between 5.518 and 7.048, which were well within the required range. It is however known that an API in its unionized form will permeate the lipid stratum corneum more

efficiently than its ionized form [45], and therefore, a lower pH value would result in a higher %unionized drug due to the pKa of diclofenac being 4.15 [46], which may lead to increased skin permeation [45], since the %unionized range is 93.3886–0.0014% for pH range of 3–9.

Nanometric droplets intended for transdermal delivery should ideally possess a droplet size < 500 nm [20, 47], which was achieved for all drug delivery vehicles. Generally, an increase in oil phase leads to an increase in droplet size [48]; nevertheless, during this study, the opposite was observed for both the NEs and NGs, where the 10% drug delivery vehicles (NE10 and NG10) displayed larger droplet sizes than the 20% drug delivery vehicles (NE20 and NG20). The aforementioned may be due to the inclusion of more surfactants (Span® 60 and Tween® 80) in the drug delivery vehicles containing more oil; hence, Hanafy et al. [49] reported that an increase in Tween® 80 concentration can result in a decrease

Fig. 1 Visual inspection of **a** CS, **b** NE10, **c** NE15, **d** NE20, **e** NG10, **f** NG15, and **g** NG20

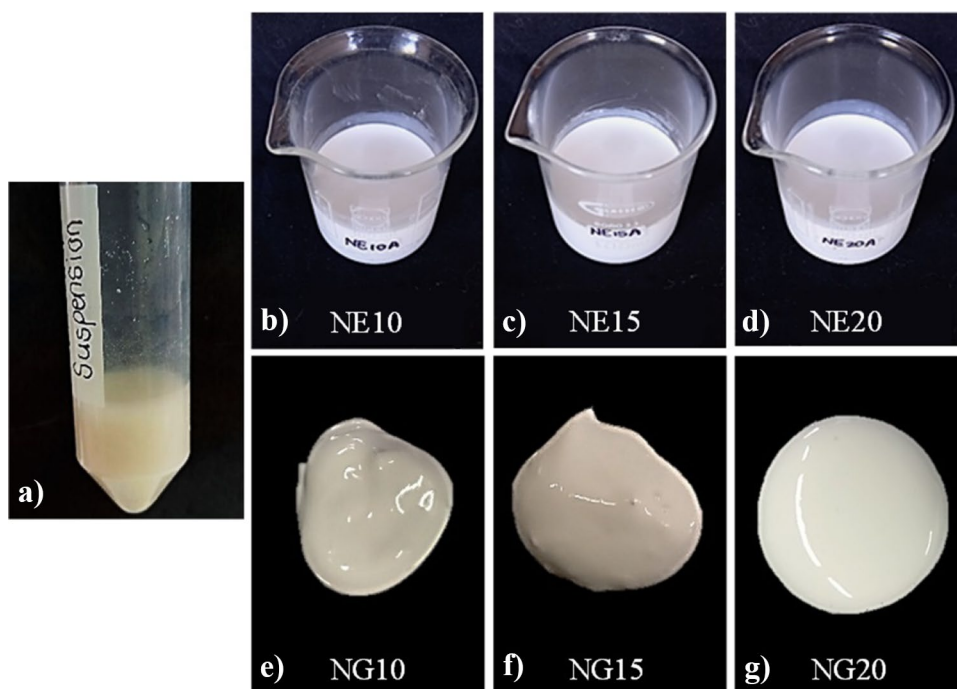
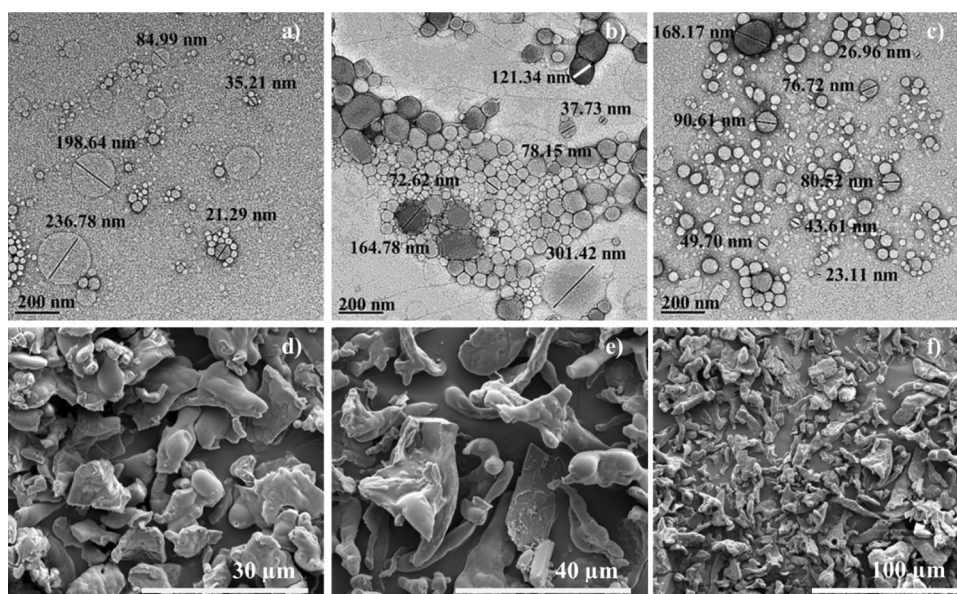


Fig. 2 TEM micrographs of the oil droplets within **a** NE10P, **b** NE15P, and **c** NE20P, together with SEM micrographs of the diclofenac-loaded NPs (**d**, **e**, and **f**)



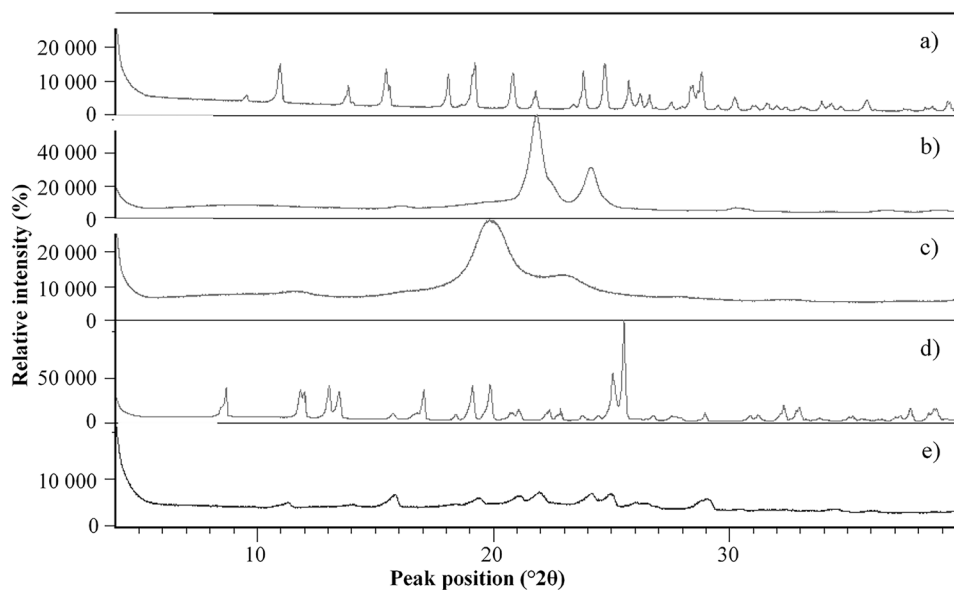
in droplet size. It was also noticeable that the NGs in comparison to the NEs counterparts had slightly higher droplet sizes, which may be due to the inclusion of Carbopol® Ultrez 20 (gelling agent). Eid et al. [50] explained that addition of Carbopol® Ultrez 20 causes the viscosity of a formulation to increase, due to a higher degree of cross-linking, which successively results in a larger droplet size. From the HRTEM micrographs (Fig. 2a–c), it is clear that the oil droplets were spherically shaped and that the oil phase was successfully dispersed to form nano-metric droplets between 50 and 200 nm [51]; although, Uchechi et al. [47] found that droplet sizes below 500 nm were still acceptable. Figure 2a–c also demonstrates that the data obtained with Malvern Zetasizer Nano ZS for the NEs containing diclofenac (NE10, NE15,

and NE20) did not differ much when compared to its placebo counterpart (NE10P, NE15P, and NE20P).

A monodispersed or a formulation that is homogenous will present with a PDI value closer to 0, whereas a poly-dispersed or a formulation that is heterogenous will have a PDI value closer to 1 [52]. Hence, the PDI values of the drug delivery vehicles were closer to 0, indicating a monodispersed sample, which may result in increased stability [53].

A zeta-potential value ranging above +30 mV or below –30 mV is necessary for increased stability [54]; hence, as observed in Table 2, all the drug delivery vehicles will have enhanced stability except for the CS, which showed a zeta-potential value closer to 0 (this corresponds with the sedimentation observed during visual inspection).

Fig. 3 XRPD overlay for **a** diclofenac, **b** PCL, **c** PVA, **d** sucrose, and **e** formulated NPs



A gelling agent (Carbopol® Ultrez 20) was added to increase the viscosity of the NEs [54], which was successfully achieved when investigating the viscosity results of the NGs in Table 2; low viscosity could cause organoleptic problems during topical/transdermal application. An increase in the EPO concentration also resulted in a viscosity increase for the NEs when looking at NE10 vs NE15 and NE20 (Table 2), since water is less viscous than EPO.

Figure 2d–f depicts SEM micrographs obtained, at different magnifications, for the synthesized, dried NPs. The SEM micrographs showed a lack of crystallinity and a fused particle morphology. From this visual observation, the crystalline habit of both sucrose and diclofenac could not be identified, and the fused morphology suggested that the NPs existed in the amorphous state.

From the diffraction patterns obtained for the individual compounds, it was possible to identify distinguishing diffraction peaks. For PCL, two distinguishing diffraction peaks at 21.85 and 24.17, PVA at 19.67, and sucrose at 25.55°2θ were identified. Although not as intense, these diffraction peaks were subsequently also identified in the diffraction pattern obtained for the NPs. With regard to the diffraction pattern of diclofenac, it was concluded to be a highly crystalline compound exhibiting several strong, unique diffraction peaks with the most significant diffraction peaks at 19.21, 23.81, 24.66, 24.74, and 28.83°2θ. These diffraction peaks were not unequivocally identifiable in the NP sample, but this may be explained by the fact that the NPs are nano-sized particles consisting of all the individual compounds (Fig. 3). It was therefore not possible to conclude on the presence of diclofenac in the NPs using PXRD analysis, but what could be confirmed was the overall lack of crystallinity of the NPs, which correlates with the SEM results.

Diffusion experiments

Only the median values (center values of distributed data) are discussed during this study since they present a more accurate description of the data, which are unaffected by outliers [55].

Membrane release

Table 3 and Fig. 4 illustrate the results from the membrane release studies.

As observed from Fig. 4, it is evident that NG15 had the lowest median flux, followed by NG20, NG10, NE15, NE20, CS, and lastly NE10 (highest median flux). It is noticeable that the NGs displayed lower median flux values when compared to that of the NEs. When the viscosity (see Table 2) of the NEs and NGs are compared, it is evident that the NGs presented with increased viscosity values, which is due to the inclusion of Carbopol® Ultrez 20 (polymer/gelling agent) in the NGs. Bolla et al. [56] found that an increase in viscosity may negatively affect API release, consequently causing lower median flux values. It is also believed that NGs may display controlled release of an API, due to its adhesive properties from the inclusion of a polymer, which may subsequently cause a slow, prolonged release rate that may contribute to lower median flux [57, 58]. While all the NEs demonstrated higher median flux values than their NGs counterparts, it should be remarked that the CS had the second highest median flux value when all the different drug delivery vehicles were compared with each other. When the median flux values of the different %EPO drug delivery vehicles (10, 15, and 20%) are compared, it is detected for both the NEs and NGs that the 10% EPO drug delivery vehicles (NE10 and NG10) had the highest median flux values, followed by the 20% EPO drug delivery vehicles (NE20 and NG20), and lastly, the 15% EPO drug delivery vehicles (NE15 and NG15). It is uncertain why a trend was not observed with regard to median flux and the %EPO in the drug delivery vehicle. Nevertheless, from the aforementioned, it was evident that the purpose of the membrane release studies was achieved, since all the drug delivery vehicles successfully released diclofenac from each respective drug delivery vehicle over the 6 h period; therefore, *in vitro* skin diffusion studies could be performed.

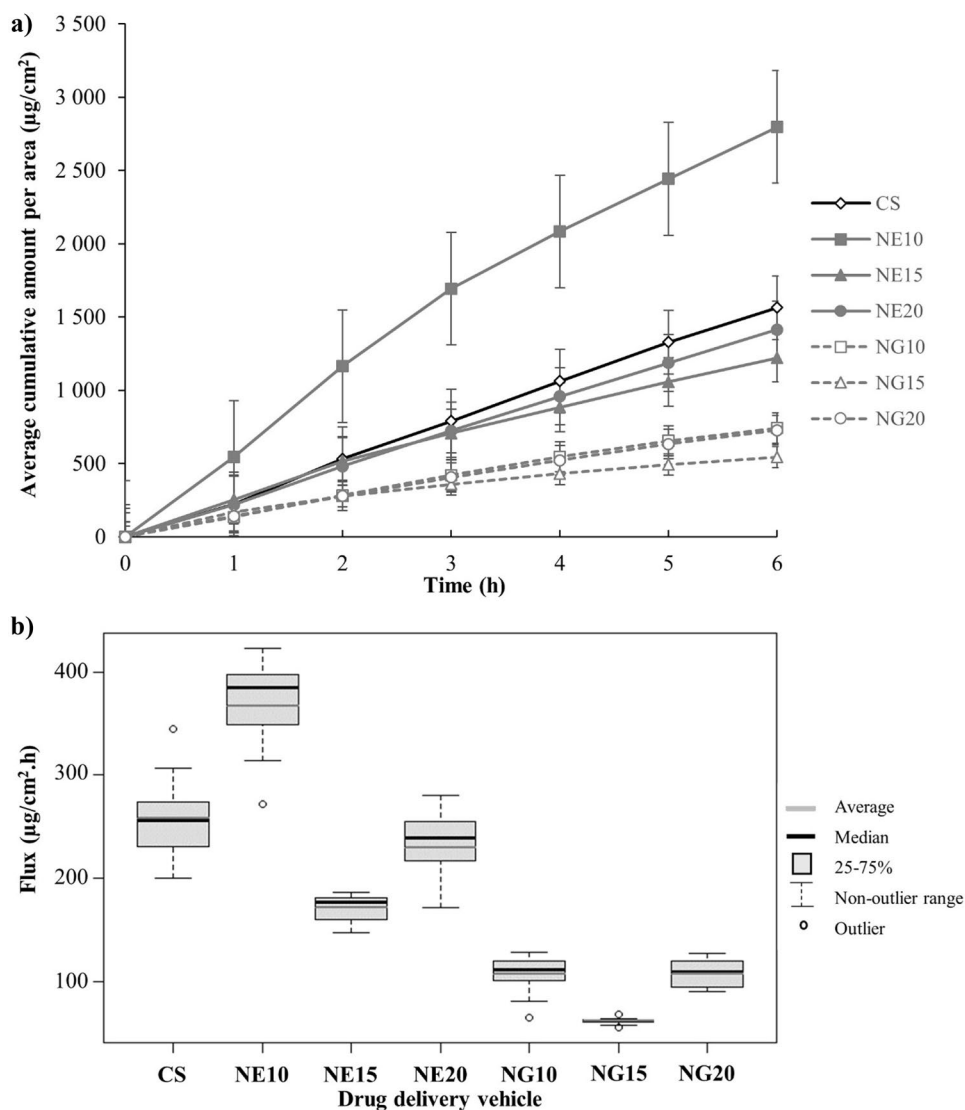
One-way ANOVA indicated a statistically significant difference in the flux values between the groups. Consequently, the Bonferroni post-hoc test investigated the differences

Table 3 Average and median flux values obtained from membrane release studies (*n* = number of Franz cells)

Drug delivery vehicle	<i>n</i>	Average released (%)	Average flux (μg/cm ² h)	Median flux (μg/cm ² h)
CS	11	6.509 ± 1.082	258.680 ± 40.616	256.089
NE10	10	11.494 ± 1.139	366.970 ± 46.059	384.670
NE15	10	5.023 ± 0.510	171.410 ± 12.927	176.611
NE20	9	5.787 ± 0.701	229.180 ± 41.112	239.087
NG10	10	3.030 ± 0.607	107.390 ± 20.202	111.560
NG15	10	2.228 ± 0.079	61.974 ± 3.344	62.313
NG20	10	2.984 ± 0.428	107.610 ± 13.016	110.005

CS colloidal suspension, NE nano-emulsion, NG nano-emulgel

Fig. 4 a Average cumulative amount of diclofenac released per area ($\mu\text{g}/\text{cm}^2$) over a period of 6 h and **b** boxplot showing the median and average flux ($\mu\text{g}/\text{cm}^2 \text{ h}$) of diclofenac released during the membrane release studies with all the drug delivery vehicles



between each of the drug delivery vehicles and showed statistically significant differences ($p < 0.001$) for all the pairwise comparisons, except for NG10 and NG20 ($p = 1.000$), together with CS and NE20 ($p = 0.633$), which showed no statistically significant difference.

In vitro skin diffusion

Table 4 and Fig. 5 illustrate the data obtained from the skin diffusion studies, which presented two median flux values with flux 1 from 0.67 to 2 h and flux 2 between 6 and 12 h.

Table 4 Average and median values of flux 1 and flux 2 obtained from skin diffusion studies (n = number of Franz cells)

Drug delivery vehicle	n	Average flux 1 ($\mu\text{g}/\text{cm}^2 \text{ h}$)	Average flux 2 ($\mu\text{g}/\text{cm}^2 \text{ h}$)	Median flux 1 ($\mu\text{g}/\text{cm}^2 \text{ h}$)	Median flux 2 ($\mu\text{g}/\text{cm}^2 \text{ h}$)
CS	10	0.3822 ± 0.236	2.2308 ± 0.272	0.310	2.273
NE10	8	6.9035 ± 2.405	5.2006 ± 0.902	5.663	4.831
NE15	10	0.3884 ± 0.093	1.3756 ± 0.209	0.372	1.355
NE20	10	0.4505 ± 0.101	1.0768 ± 0.136	0.442	1.058
NG10	10	2.9430 ± 1.340	4.3370 ± 0.742	2.334	4.307
NG15	7	0.0832 ± 0.022	0.7128 ± 0.053	0.085	0.729
NG20	10	0.4425 ± 0.128	0.9588 ± 0.098	0.428	0.932

CS colloidal suspension, NE nano-emulsion, NG nano-emulgel

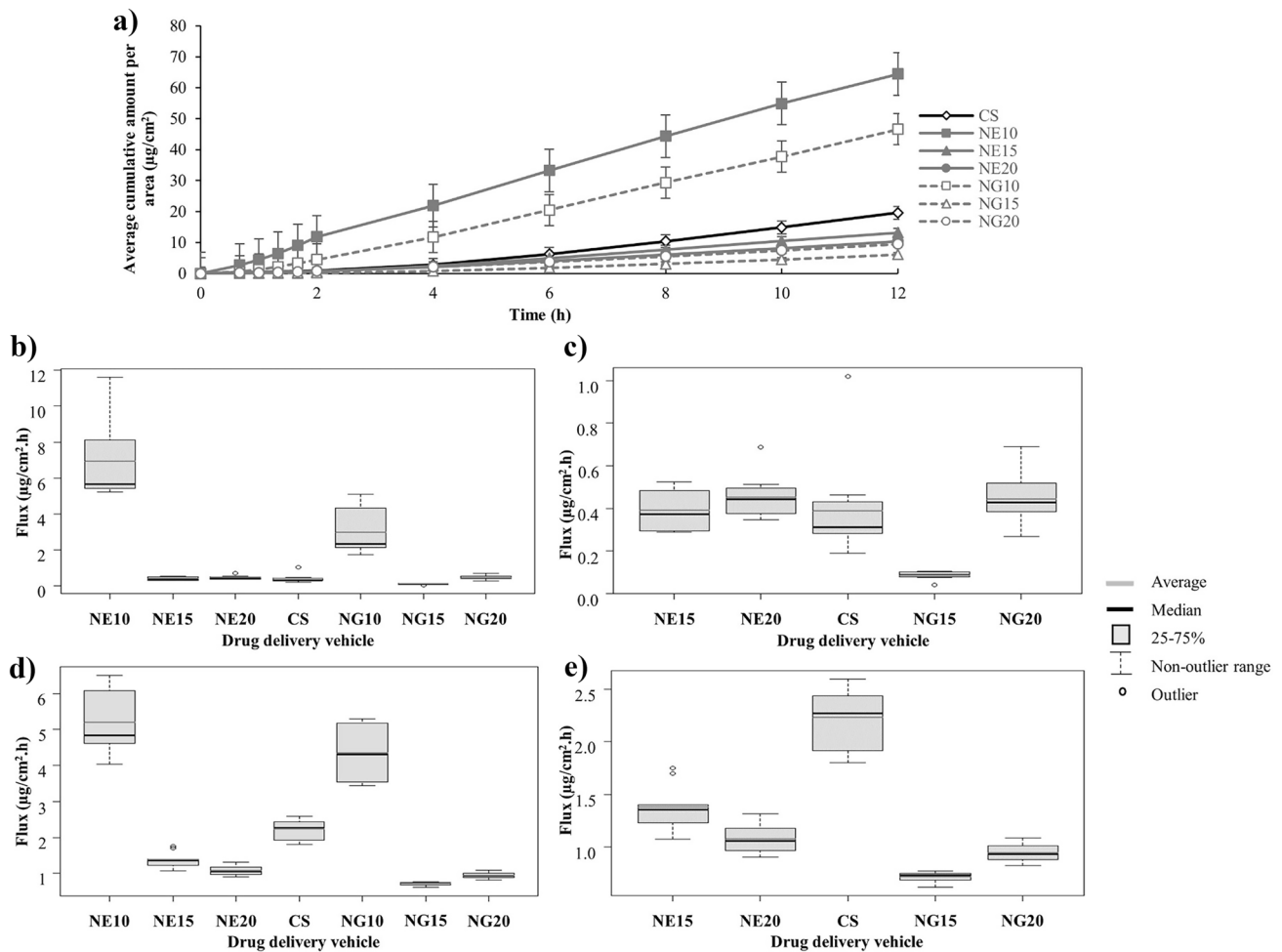


Fig. 5 **a** Average cumulative amount of diclofenac diffused per area ($\mu\text{g}/\text{cm}^2$) over a period of 12 h and **b–e** boxplots showing the median and average flux ($\mu\text{g}/\text{cm}^2\cdot\text{h}$) of diclofenac, where **b** is flux 1 ($\mu\text{g}/\text{cm}^2\cdot\text{h}$) at 0.67–2 h, and **c** is an extraction of **b** flux 1, while **d** is flux 2

($\mu\text{g}/\text{cm}^2\cdot\text{h}$) at 6–12 h, and **e** is an extraction of **d** flux 2 that diffused during the in vitro skin diffusion studies with all the drug delivery vehicles

The results indicated that NE10 obtained the highest median flux 1 followed by NG10, NE20, NG20, NE15, CS, and lastly, NG15. A similar trend was observed for median flux 2, except for CS and NE15, which showed improved transdermal diffusion after 2 h.

For both median flux 1 and median flux 2, the NEs obtained enhanced skin diffusion when compared to their NG counterparts. The inclusion of a gelling agent when formulating NGs increases viscosity, and though very controversial, it may appear that the increase in viscosity may have slightly decreased skin diffusion when the NEs are compared to the NG counterparts; however, the inclusion of a polymer/gelling agent (such as Carbopol® Ultrez 20) may result in a film-forming effect that allows for a slow and constant controlled permeation of the API through the skin [57, 58], which may cause a lower median flux (rate of diffusion) than its NE counterpart during the first 12 h of diffusion.

A trend is observed when the different %EPO vehicles (10, 15, and 20%) are compared, since the 10% EPO vehicles (NE10 and NG10) achieved the highest median flux, followed by the 20% EPO vehicles (NE20 and NG20), and lastly, the 15% EPO vehicles (NE15 and NG15), except for NE15, which presented with a higher median flux than the 20% EPO vehicles at flux 2 (between 2.00 and 12.00 h). According to literature, formulations with lower oil concentrations (i.e., NE10 and NG10) have improved skin permeation [54, 59], while formulations with increased surfactant and high oil concentrations (like NE15, NG15, NE20, and NG20 in comparison to NE10 and NG10) may result in decreased transdermal delivery due to irritation caused by the surfactants [60]. Surfactants also influence skin permeation in a concentration-dependent manner, where low surfactant concentrations increase skin permeability, and the opposite is true for high surfactant

concentrations [61]. Hence, it is observed that this is not true when the 15% EPO vehicles (NE15 and NG15) and 20% EPO vehicles (NE20 and NG20) are compared, except if the amount of Span® 60 (more than the total amount of surfactants or the amount of Tween® 80) included during formulation had a greater influence on skin permeation. If low oil and low surfactant concentrations are not taken into account and formulations with higher oil and higher surfactant concentrations are compared, there is a possibility that pH may have an influence on drug delivery, since (in the case of diclofenac) a lower pH (see Table 2) will result in a higher %unionized drug, leading to improved skin permeation [45]. Therefore, in this study, it seems that the film-forming effect has an influence on median flux (skin diffusion) when the NEs and NGs are compared, while the oil and surfactant concentrations in the drug delivery vehicles had a greater influence than the pH when the %EPO vehicles are compared.

Focusing on the CS, it should however be noted that the CS contained no penetration enhancers, gelling agents, or stabilizers, yet still successfully delivered diclofenac through the skin. The CS initially had a low median flux 1 (0.67–2 h), which improved after 2 h (flux 2), indicating the slow and controlled release of diclofenac, commonly found in NPs [62, 63]. The NPs are reportedly transported through the hair follicles [64], where it accumulates within the lower region of the infundibulum [65] and causes a depot effect [66, 67], which may explain the observed increase in median flux from flux 1 to flux 2. Since diclofenac is readily available from the saturated infundibulum, the hair follicle can deliver it into the systemic circulation (due to the middle vascular plexus surrounding the hair follicles), which will lead to increased API delivery [68, 69]. The low-median flux 1 value can thus possibly be due to the ongoing accumulation of the NPs that have not yet saturated the hair follicle.

The one-way ANOVA performed on the groups of the two fluxes indicated the differences were statistically significant ($p < 0.001$ for flux 1 and flux 2). The Bonferroni

post-hoc test was for multiple comparisons of the different groups and indicated statistically significant differences at both the flux 1 and flux 2 groups, except for the following groups, which showed no statistically significant differences at flux 1: CS and NG20 ($p = 1.000$), CS and NE20 ($p = 1.000$), CS and NE15 ($p = 1.000$), NE15 and NG20 ($p = 1.000$), NE15 and NE20 ($p = 1.000$), together with NE20 and NG20 ($p = 1.000$) and at flux 2: NE10 and NG10 ($p = 0.140$), together with NE20 and NG20 ($p = 0.891$).

Tape stripping

Table 5 displays the concentrations of diclofenac obtained within the SCE and ED from the different drug delivery vehicles.

The CS had the highest median concentration of diclofenac in the SCE, followed by NE10, NG10, NE20, NE15, NG15, and lastly, NG20, while a similar trend was observed for the ED, except for NG15 and NG20.

The CS had the highest concentration within the SCE and ED indicating that a large concentration of diclofenac resided in the skin (topically). Apart from following the transfollicular route [64], the hydration of the skin during skin diffusion studies [70] could have allowed the CS (which is more hydrophilic in nature in comparison to the other drug delivery vehicles containing an oil phase) to accumulate in the skin once the hair follicles became oversaturated, and the NPs had to seek alternative pathways for the permeation.

The NEs showed higher API concentrations within the skin than their NG counterparts, which may be ascribed to the larger droplet sizes of the NGs that decrease permeation into the stratum corneum. The inclusion of a gelling agent (which may have a film-forming effect) during the formulation of the NG can further decrease permeation due to a slower release of the API caused by a more structured packing of the oil droplets in the NGs in comparison to the NEs [54, 57, 58].

Table 5 Tape stripping data of the different drug delivery vehicles

Drug delivery vehicle	Average concentration in SCE (µg/ml)	Median concentration in SCE (µg/ml)	Average concentration in ED (µg/ml)	Median concentration in ED (µg/ml)
CS	50.434 ± 17.244	45.641	29.231 ± 13.275	28.072
NE10	3.275 ± 1.233	3.103	8.837 ± 8.536	5.663
NE15	1.479 ± 0.315	1.481	1.463 ± 0.181	1.474
NE20	1.913 ± 1.025	1.695	2.013 ± 0.562	1.821
NG10	2.916 ± 0.709	2.798	5.450 ± 3.750	4.855
NG15	1.098 ± 0.163	1.079	1.039 ± 0.486	0.903
NG20	0.443 ± 0.267	0.373	1.201 ± 0.609	0.961

CS colloidal suspension, ED epidermis-dermis, NE nano-emulsion, NG nano-emulgel, SCE stratum corneum-epidermis

The 10% EPO drug delivery vehicles also showed increased skin (topical) permeation when compared to those with higher %EPO. It should be noted that the 15 and 20% EPO drug delivery vehicles consist of a smaller water phase due to their larger concentration of EPO. Hence, the drug delivery vehicles with lower viscosity and lower oil concentrations demonstrated improved skin permeation [54, 59, 71].

It is clearly observed that the API permeated the hydrophilic ED and did not remain in the SCE indicating that the lipid matrix barrier of the SCE was successfully overcome. Furthermore, the increased API concentration within the SCE observed for the 10% EPO drug delivery vehicles could have increased API concentrations within the ED, due to the concentration gradient acting as a driving force [72]. Of note, the lipophilic nature of diclofenac contributes to the permeation of the API into the lipophilic SCE [73].

There were two variables considered during the statistical analysis of the tape stripping data, which included the drug delivery vehicles and the tape stripping data (SCE and ED). The *F*-test showed statistically significant differences for the drug delivery vehicles ($p < 0.001$) and the tape stripping data ($p = 0.002$). The *F*-test *p*-value for the interaction effect between the two variables also proved statistically significant ($p < 0.001$). The *p*-values between the drug delivery vehicles were determined and indicated no statistically significant difference between the following groups within the SCE: NE10 and NG10, NE10 and NE20, NE15 and NG15, NE15 and NE20, NE20 and NG15, together with NE20 and NG10, or within the ED: NE20 and NE15, NG10 and NE10, NG15 and NE15, NG20 and NG15, NG20 and NE20, together with NG20 and NE15. A comparison between the concentrations in the SCE and the ED within each delivery

vehicle showed no statistically significant difference for NE15, NE20, and NG15. All the other pairwise comparisons proved to have statistically significant differences [74].

Cytotoxicity

Figure 6a and b shows the regression curve for the diclofenac solution, NE10, and NE10P, while Fig. 6c and d depicts the regression curve obtained for the NPs from the cytotoxicity studies. Table 6 lists the IC_{50} values obtained from MTT and NR assays of the diclofenac solution, NE10, NE10P, and the NPs.

The IC_{50} values of the MTT assays indicated that the NPs had the most cytotoxic effect, as a lower concentration is required to inhibit the growth of 50% of the cells; contrarily, diclofenac (solution) requires a higher concentration to inhibit 50% of the cells and is therefore less cytotoxic. The IC_{50} values of the NR assay indicated that NE10 had the highest cytotoxic effects and diclofenac (solution) the lowest.

The level of cytotoxicity can be indicated by the %cell viability, where strong cytotoxic effects are observed with a cell viability below 40%, moderate cytotoxicity between 40 and 60%, weak cytotoxicity between 60 and 80%, and no cytotoxicity above 80% [75]. During the MTT assay, the diclofenac solution and NE10P only showed moderate cytotoxicity at the highest treatment concentrations, whereas NE10 showed strong cytotoxic effects. These concentrations were, however, above the concentrations detected during the in vitro skin diffusion studies.

NE10 and NE10P displayed strong cytotoxic effects at high treatment concentrations during the NR assay. There was weak cytotoxicity observed at the high treatment concentrations of the diclofenac solution.

Fig. 6 %Cell viability of the HaCaT cells after a 12-h exposure period with the different concentrations of the diclofenac solution, NE10, and NE10P treatments as determined with **a** MTT assay and **b** NR assay and for different concentrations of the NPs treatment during the **c** MTT-assay and **d** NR-assay. All the data were normalized to the untreated control, which is considered as 100% viable

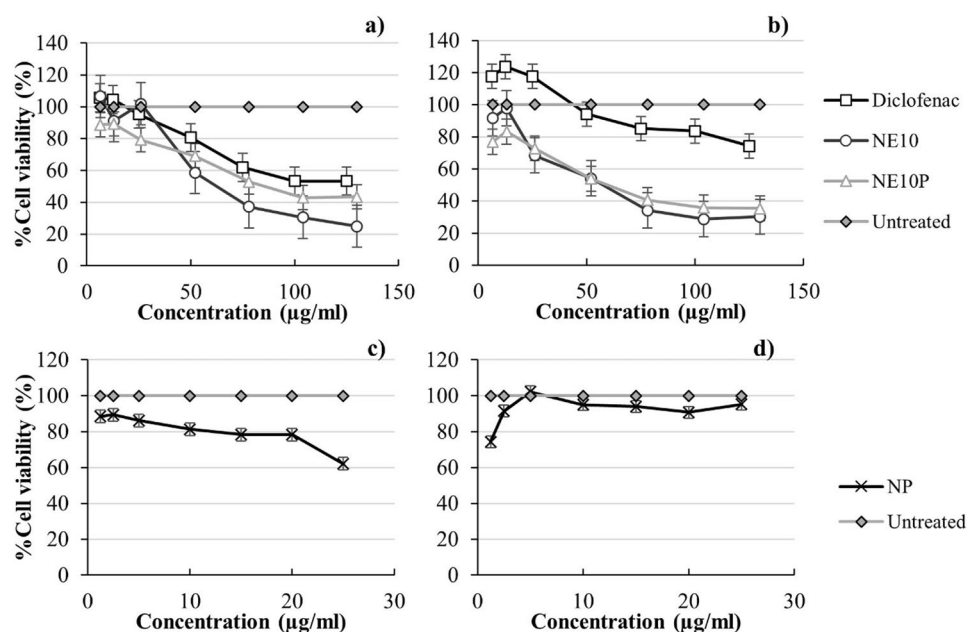


Table 6 IC_{50} values for the various treatment groups obtained by using the MTT and NR assays

Treatment group	IC_{50} value ($\mu\text{g/ml}$)	
	MTT assay	NR assay
Diclofenac	114.917	174.790
NE10	78.801	72.297
NE10P	97.845	75.331
NPs	43.200	Inconclusive

MTT methyl thiazolyl tetrazolium, NE nano-emulsion, NP nanoparticle, NR neutral red

The conclusion is that the treatment groups showed minimum cytotoxic effects at the treatment concentrations equivalent to those that permeated through the skin during diffusion studies. The increased cytotoxicity of the NE10 and NE10P, compared to the diclofenac solution, may be due to the inclusion of other excipients within the drug delivery vehicles (such as EPO, Tween[®] 80, and Span[®] 60). These excipients may lead to increased cytotoxicity by hindering the gas diffusion of cells [60]. Place et al. [76] have shown that cells experience restricted gas exchange in a thick medium, of which nano-emulsions have this characteristic.

Conclusion

All the drug delivery vehicles successfully permeated the skin to deliver diclofenac systemically at concentrations proven to be non-cytotoxic.

Overall, the CS had the highest concentrations in the SCE and ED, the second-highest API release, and the third-highest median flux 2 value despite having a low significant median flux 1. The accumulation of NPs in the hair follicle over time may have produced a depot effect, which allowed for a more regulated release of diclofenac. This depot effect may have contributed to the enhanced delivery of diclofenac over time. Furthermore, the NEs outperformed the NGs during the release, topical, and transdermal delivery of diclofenac. When NEs are compared to gel-like formulations, research shows that the NEs exhibit enhanced diffusion with steady-state fluxes. This might be due to the addition of a gelling agent in NGs that produces a film-forming effect which slows the release of the API. The 10% EPO drug delivery vehicles (NE10 and NG10) were found to be superior in all cases in comparison to the other EPO drug delivery vehicles. The 20% EPO drug delivery vehicles (NE20 and NG20) showed improved results compared to the 15% EPO drug delivery vehicles (apart from the NG20 in the SCE and NE15 during the median flux 2 results).

It could be concluded from the topical and transdermal results that the type of drug delivery vehicle and the %EPO incorporated into the drug delivery vehicles can have a definite effect on the skin permeation and diffusion of diclofenac.

For future, researchers could consider adding a gelling agent to the CS to produce a hydrogel. Furthermore, diclofenac salts with increased solubility can be used and compared to diclofenac acid (2-[2-(2,6-dichloroanilino) phenyl] acetic acid).

Acknowledgements A sincere word of appreciation to Dr. Marike Cockeran at the Statistical Consultation Services, North-West University (NWU), for the statistical data analysis and Prof. Frank van der Kooy from the Analytical Technology Laboratory (ATL), Pharmacen[™], NWU for his excellent guidance during HPLC method validation. Dr. Anine Jordaan from the Laboratory for Electron Microscopy (LEM), Chemical Resource Beneficiation, NWU, performed the transmission electron microscopy (TEM) and scanning electron microscopy (SEM) analysis.

Author contribution E-VL performed the experiments, interpreted the results, and drafted the original manuscript. MG, WL, and MEA supervised, attained funding for the project, and assisted in writing the manuscript through critical reviewing and editing. MG conceptualized and designed the project. CW maintained the in vitro cell cultures and assisted with the cytotoxicity experiments. AD provided assistance and critical input into the formulation of drug delivery vehicles, especially the nanoparticles. All authors have read, edited, and approved the final version of the manuscript.

Funding The authors express gratitude to the research funds of Prof. M. Gerber and The Centre of Excellence for Pharmaceutical Sciences (Pharmacem[™]) of the North-West University (NWU), South Africa, for the financial support and facilities provided to complete this study.

Availability of data and materials The datasets generated during and/or analyzed during the current study are available from the corresponding author on reasonable request.

Declarations

Ethical approval and consent to participate The study was approved by the North-West University Health Research Ethics Committee (NWU-HREC) (Ethics approval no: NWU-00111–17-A1-10) and conformed with the Declaration of Helsinki. Written informed consent was obtained from each patient.

Consent for publication All the authors gave their consent for publication of this manuscript in the CRS Local Chapter Special Issue of Drug Delivery and Translational Research (DDTR). Although informed consent was attained from all participants, the manuscript contains no personal data of any participant in any form. No children were included in the study.

Conflict of interest The authors declare no competing interests.

References

- Chen H, Khemtong C, Yang X, Chang X, Gao J. Nanonization strategies for poorly water-soluble drugs. *Drug Discov Today*. 2011;16:354–60. <https://doi.org/10.1016/j.drudis.2010.02.009>.

2. Yaksh TL, Woller SA, Ramachandran R, Sorkin LS. The search for novel analgesics: targets and mechanisms. *F1000Prime Rep*. 2015;7:56. <https://doi.org/10.12703/P7-56>
3. Brandolini L, Grannonico M, Bianchini G, Colanardi A, Sebastiani P, Paladini A, Piroli A, Allegretti M, Varrassi G, Di Loreto S. The novel C5aR antagonist DF3016A protects neurons against ischemic neuroinflammatory injury. *Neurotox Res*. 2019;36:163–74. <https://doi.org/10.1007/s12640-019-00026-w>.
4. Fusco M, Skaper SD, Coaccioli S, Varrassi G, Paladini A. Degenerative joint diseases and neuroinflammation. *Pain Pract*. 2017;17:522–32. <https://doi.org/10.1111/papr.12551>.
5. Varrassi G, Alon E, Bagnasco M, Lanata L, Mayoral-Rojals V, Paladini A, Pergolizzi JV, Perrot S, Scarpignato C, Tölle T. Towards an effective and safe treatment of inflammatory pain: a Delphi-guided expert consensus. *Adv Ther*. 2019;36:2618–37. <https://doi.org/10.1007/s12325-019-01053-x>.
6. Skoutakis VA, Carter CA, Mickle TR, Smith VH, Arkin CR, Alissandratos J, Petty DE. Review of diclofenac and evaluation of its place in therapy as a nonsteroidal antiinflammatory agent. *Drug Intell Clin Pharm*. 1988;22:850–9. <https://doi.org/10.1177/106002808802201102>.
7. Osafo N, Agyare C, Obiri DD, Antwi AO. Mechanism of action of nonsteroidal antiinflammatory drugs. In: Al-kaf AGA, editor. *Nonsteroidal anti-inflammatory drugs*. London: IntechOpen; 2017. <https://www.intechopen.com/chapters/55279>. Accessed 20 Jun 2022. <https://doi.org/10.5772/68090>
8. Altman R, Bosch B, Brune K, Patrignani P, Young C. Advances in NSAID development: evolution of diclofenac products using pharmaceutical technology. *Drugs*. 2015;75:859–77. <https://doi.org/10.1007/s40265-015-0392-z>.
9. Subedi RK, Oh SY, Chun M-K, Choi H-K. Recent advances in transdermal drug delivery. *Arch Pharm Res*. 2010;33:339–51. <https://doi.org/10.1007/s12272-010-0301-7>.
10. Flynn GL. Cutaneous and transdermal delivery - processes and system of delivery. In: Banker GS, Rhodes CT, editors. *Modern Pharmaceutics*. Boca Raton: CRC Press; 2002. p. 187–235.
11. Kala S, Juyal D. Recent developments on natural transdermal penetration enhancers. *Int J Pharm Sci Res*. 2018;9:2190–6. [https://doi.org/10.13040/IJPSR.0975-8232.9\(6\).2190-96](https://doi.org/10.13040/IJPSR.0975-8232.9(6).2190-96)
12. Bouwstra JA, Ponc M. The skin barrier in healthy and diseased state. *Biochim Biophys Acta*. 2006;1758:2080–95. <https://doi.org/10.1016/j.bbame.2006.06.021>.
13. El Maghraby GM, Barry BW, Williams AC. Liposomes and skin: from drug delivery to model membranes. *Eur J Pharm Sci*. 2008;34:203–22. <https://doi.org/10.1016/j.ejps.2008.05.002>.
14. Naik A, Kalia YN, Guy RH. Transdermal drug delivery: overcoming the skin's barrier function. *Pharm Sci Technol Today*. 2000;3:318–26. [https://doi.org/10.1016/s1461-5347\(00\)00295-9](https://doi.org/10.1016/s1461-5347(00)00295-9).
15. Williams AC. Theoretical aspects of transdermal drug delivery. In: Williams AC, editor. *Transdermal and topical drug delivery: from theory to clinical practice*. London: Pharmaceutical Press; 2003. p. 27–50.
16. Williams AC. Topical and transdermal drug delivery. In: Aulton ME, editor. *Aulton's Pharmaceutics: the design and manufacture of medicines*. London: Churchill Livingstone; 2013. p. 675–97.
17. Büyüktimkin N, Büyüktimkin S, Rytting JH. Chemical means of drug permeation enhancement. In: Ghosh TK, Pfister WR, Yum SII, editors. *Transdermal and topical drug delivery systems*. Buffalo Grove: Interpharm Press; 1997. p. 357–475.
18. Gupta A. Nanoemulsions. In: Chung EJ, Leon L, Rinaldi C, editors. *Nanoparticles for biomedical applications: fundamental concepts, biological interactions and clinical applications*. Amsterdam: Elsevier; 2020. pp. 371–84. <https://doi.org/10.1016/B978-0-12-816662-8.00021-7>
19. Mukherjee PK, Harwansh RK, Bhattacharyya S. Bioavailability of herbal products: approach toward improved pharmacokinetics. In: Mukherjee PK, editor. *Evidence-based validation of herbal medicine*. Amsterdam: Elsevier; 2015. pp. 217–45. <https://doi.org/10.1016/B978-0-12-800874-4.00010-6>
20. Yu Y-Q, Yang X, Wu X-F, Fan Y-B. Enhancing permeation of drug molecules across the skin via delivery in nanocarriers: novel strategies for effective transdermal applications. *Front Bioeng Biotechnol*. 2021. <https://doi.org/10.3389/fbioe.2021.646554>.
21. Souto EB, Cano A, Martins-Gomes C, Coutinho TE, Zielińska A, Silva AM. Microemulsions and nanoemulsions in skin drug delivery. *Bioengineering*. 2022;9:158. <https://doi.org/10.3390/bioengineering9040158>.
22. Flourey J, Desrumaux A, Lardières J. Effect of high-pressure homogenization on droplet size distributions and rheological properties of model oil-in-water emulsions. *Innov Food Sci Emerg Technol*. 2000;1:127–34. [https://doi.org/10.1016/S1466-8564\(00\)00012-6](https://doi.org/10.1016/S1466-8564(00)00012-6).
23. Shehata TM, Elnahas HM, Elsewedy HS. Development, characterization and optimization of the anti-inflammatory influence of meloxicam loaded into a eucalyptus oil-based nanoemulgel. *Gels*. 2022;8:262. <https://doi.org/10.3390/gels8050262>.
24. Barnes TM, Mijaljica D, Townley JP, Spada F, Harrison IP. Vehicles for drug delivery and cosmetic moisturizers: review and comparison. *Pharmaceutics*. 2021;13:2012. <https://doi.org/10.3390/pharmaceutics13122012>.
25. Miastkowska M, Kulawik-Pióro A, Szczurek M. Nanoemulsion gel formulation optimization for burn wounds: analysis of rheological and sensory properties. *Processes*. 2020;8:1416. <https://doi.org/10.3390/pr8111416>.
26. Jantrawut P, Ruksiriwanich W. Carbopol®-guar gum gel as a vehicle for topical gel formulation of pectin beads loaded with rutin. *Asian J Pharm Clin Res*. 2014;7:231–6. <https://innovareacademics.in/journals/index.php/ajpcr/article/view/2741/1168>. Accessed 20 Jun 2022.
27. Lubrizol Advanced Materials, Inc. - Technical data sheet: neutralizing Carbopol®* and Pemulen™* polymers in aqueous and hydroalcoholic systems. 2009. https://www.lubrizol.com/-/media/Lubrizol/Health/TDS/TDS-237_Neutralizing_Carbopol_Pemulen_in_Aqueous_Hydroalcoholic_Systems--PH.pdf. Accessed 20 Jun 2022.
28. Boltachev GSh, Ivanov MG. Effect of nanoparticle concentration on coagulation rate of colloidal suspensions. *Heliyon*. 2020;6:e03295. <https://doi.org/10.1016/j.heliyon.2020.e03295>.
29. Buzea C, Pacheco II, Robbie K. Nanomaterials and nanoparticles: sources and toxicity. *Biointerphases*. 2007;2:MR17–71. <https://doi.org/10.1116/1.2815690>
30. Zhang Z, Tsai P-C, Ramezani T, Michniak-Kohn BB. Polymeric nanoparticles-based topical delivery systems for the treatment of dermatological diseases. *WIREs Nanomed Nanobiotechnol*. 2013;5:205–18. <https://doi.org/10.1002/wnan.1211>.
31. Gaber M, Medhat W, Hany M, Saher N, Fang JY, Elzoghby A. Protein-lipid nanohybrids as emerging platforms for drug and gene delivery: challenges and outcomes. *J Control Release*. 2017;254:75–91. <https://doi.org/10.1016/j.jconrel.2017.03.392>.
32. Zhang Q, Murawsky M, LaCount T, Hao J, Kasting GB, Newman B, Ghosh P, Raney SG, Li SK. Characterization of temperature profiles in skin and transdermal delivery system when exposed to temperature gradients in vivo and in vitro. *Pharm Res*. 2017;34:1491–504. <https://doi.org/10.1007/s11095-017-2171-x>.
33. Sithole MN, Marais S, Maree SM, Du Plessis LH, Du Plessis J, Gerber M. Development and characterization of nano-emulsions and nano-emulgels for transdermal delivery of statins. *Expert Opin Drug Deliv*. 2021;18:789–801. <https://doi.org/10.1080/17425247.2021.1867533>.
34. Goyal R, Macri LK, Kaplan HM, Kohn J. Nanoparticles and nanofibers for topical drug delivery. *J Control Release*. 2016;240:77–92. <https://doi.org/10.1016/j.conrel.2015.10.049>.
35. Ndumiso M, Buchtová N, Husselmann L, Mohamed G, Klein A, Aucamp M, Canevet D, D'Souza S, Maphasa RE, Boury F,

- Dube A. Comparative whole corona fingerprinting and protein adsorption thermodynamics of PLGA and PCL nanoparticles in human serum. *Colloids Surf B Biointerfaces*. 2020;188:110816. <https://doi.org/10.1016/j.colsurfb.2020.110816>.
36. Fox LT, Mazumder A, Dwivedi A, Gerber M, Du Plessis J, Hamman JH. In vitro wound healing and cytotoxicity activity of the gel and whole-leaf materials from selected aloe species. *J Ethnopharmacol*. 2017;200:1–7. <https://doi.org/10.1016/j.jep.2017.02.017>.
 37. Fouché M, Willers C, Hamman S, Malherbe C, Steenekamp J. Wound healing effects of Aloe muth-muth: in vitro investigations using immortalized human keratinocytes (HaCaT). *Biology*. 2020;9:350. <https://doi.org/10.3390/biology9110350>.
 38. Wentzel JF, Lewies A, Bronkhorst AJ, Van Dyk E, Du Plessis LH, Pretorius PJ. Exposure to high levels of fumarate and succinate leads to apoptotic cytotoxicity and altered global DNA methylation profiles in vitro. *Biochimie*. 2017;135:28–34. <https://doi.org/10.1016/j.biochi.2017.01.004>.
 39. Indrayanto G, Putra GS, Suhud F. Validation of in-vitro bioassay methods: application in herbal drug research. In: Al-Majed AA, editor. Profiles of drug substances, excipients and related methodology. Cambridge: Elsevier; 2021. pp. 273–307. <https://doi.org/10.1016/bs.podrm.2020.07.005>
 40. N'Da DD. Prodrug strategies for enhancing the percutaneous absorption of drugs. *Mol*. 2014;19:20780–807. <https://doi.org/10.3390/molecules191220780>.
 41. Dahiru T. P-value a true test of statistical significance? A cautionary note. *Ann Ib Postgrad Med*. 2008;6:21–6. <https://doi.org/10.4314/aipm.v6i1.64038>.
 42. Collier SW, Bronaugh RL. Receptor fluids. In: Bronaugh RL, Maibach HI, editors. In vitro percutaneous absorption: principles fundamentals and applications. Boca Raton: CRC Press; 1991. p. 31–49.
 43. Bhal SK. LogP—Making sense of the value. *Advanced Chemistry Development, Inc: Toronto*. 2007. https://www.acdlabs.com/wp-content/uploads/2022/02/making_sense.pdf. Accessed 24 Jun 2022.
 44. Barry B. Transdermal drug delivery. In: Aulton ME, editor. Aulton's pharmaceutics: the design and manufacture of medicines. London: Churchill Livingstone; 2002. p. 499–533.
 45. Akula P, Lakshmi PK. Effect of pH on weakly acidic and basic model drugs and determination of their ex vivo transdermal permeation routes. *Braz J Pharm Sci*. 2018;54: e00070. <https://doi.org/10.1590/s2175-97902018000200070>.
 46. Davies NM, Anderson KE. Clinical pharmacokinetics of diclofenac. *Clin Pharmacokinet*. 1997;33:184–213. <https://doi.org/10.2165/00003088-199733030-00003>.
 47. Uchechi O, Ogbonna JDN, Attama AA. Nanoparticles for dermal and transdermal drug delivery. In: Sezer AD, editor. Application of nanotechnology in drug delivery. London: IntechOpen; 2014. <https://www.intechopen.com/chapters/47025>. Accessed 24 Jun 2022. <https://doi.org/10.5772/58672>
 48. Yaping A, Xiangxing Y, Bin Li YL. Microencapsulation of capsaicin by self-emulsifying nano-emulsions and stability evaluation. *Eur Food Res Technol*. 2014;239:1077–85.
 49. Hanafy AS, Farid RM, ElGamal S. Complexation as an approach to entrap cationic drugs into cationic nanoparticles administered intra-nasally for Alzheimer's disease management: preparation and detection in rat brain. *Drug Dev Ind Pharm*. 2015;41:2055–68. <https://doi.org/10.3109/03639045.2015.1062897>.
 50. Eid AM, El-Enshasy HA, Aziz R, Elmarzugi NA. Preparation, characterization and anti-inflammatory activity of Swietenia macrophylla nanoemulgel. *J Nanomed Nanotechnol*. 2014;5:1–10. <https://doi.org/10.4172/2157-7439.1000190>.
 51. Tados T, Izquierdo P, Esquena J, Solans C. Formation and stability of nano-emulsions. *Adv Colloid Interface Sci*. 2004;108–9:303–18. <https://doi.org/10.1016/j.cis.2003.10.023>.
 52. Gaumet M, Vargas A, Gurny R, Delie F. Nanoparticles for drug delivery: the need for precision in reporting particle size parameters. *Eur J Pharm Biopharm*. 2008;69:1–9. <https://doi.org/10.1016/j.ejpb.2007.08.001>.
 53. Chime SA, Kenechukwu FC, Attama AA. Nanoemulsions – advances in formulation, characterization and applications in drug delivery. In: Sezer AD, editor. Application of nanotechnology in drug delivery. London: IntechOpen; 2014. <https://www.intechopen.com/chapters/47116>. Accessed 24 Jun 2022. <https://doi.org/10.5772/58673>
 54. Schreiner TB, Santamaria-Echart A, Ribeiro A, Peres AM, Dias MM, Pinho SP, Barreiro MF. formulation and optimization of nanoemulsions using the natural surfactant saponin from Quillaja bark. *Molecules*. 2020;25:1538. <https://doi.org/10.3390/molecules25071538>.
 55. Dawson B, Trap RG. Summarizing data and presenting data in tables and graphs. In: Dawson B, Trap RG, editors. Basic and clinical biostatistics. New York: Lange Medical Books/McGraw-Hill; 2004. p. 30–9.
 56. Bolla PK, Clark BA, Juluri A, Cheruvu HS, Renukuntla J. Evaluation of formulation parameters on permeation of ibuprofen from topical formulations using Strat-M® membrane. *Pharmaceutics*. 2020;12(2):151. <https://doi.org/10.3390/pharmaceutics12020151>.
 57. Tran TTD, Tran PHL. Controlled release film forming systems in drug delivery: the potential for efficient drug delivery. *Pharmaceutics*. 2019;11(6):290. <https://doi.org/10.3390/pharmaceutics11060290>.
 58. Dhawan VV, Nagarsenker MS. Cationic systems in nanotherapeutics – biophysical aspects and novel trends in drug delivery applications. *J Contr Release*. 2017;266:331–45. <https://doi.org/10.1016/j.jconrel.2017.09.040>.
 59. Shakeel F, Baboota S, Ahuja A, Ali J, Aqil M, Shafiq S. Nanoemulsions as vehicles for transdermal delivery of aceclofenac. *AAPS PharmSciTech*. 2007;8:191. <https://doi.org/10.1208/pt0804104>.
 60. Stockert JC, Blázquez-Castro A, Cañete M, Horobin RW, Villanueva Á. MTT assay for cell viability: intracellular localization of the formazan product is in lipid droplets. *Acta Histochem*. 2012;114:785–96. <https://doi.org/10.1016/j.acthis.2012.01.006>.
 61. Scheuplein RJ, Ross L. Effects of surfactants and solvents on the permeability of epidermis. *J Soc Cosmet Chem*. 1970;21:853–73.
 62. Ghadiri M, Vasheghani-Farahani E, Atyabi F, Kobarfard F, Mohamadyar-Toupkanlou F, Hosseinkhani H. Transferrin-conjugated magnetic dextran-spermine nanoparticles for targeted drug transport across blood-brain barrier. *J Biomed Mater Res A*. 2017;105:2851–64. <https://doi.org/10.1002/jbm.a.36145>.
 63. Soliman G. Nanoparticles as safe and effective delivery systems of antifungal agents: achievements and challenges. *Int J Pharm*. 2017;523:15–32. <https://doi.org/10.1016/j.ijpharm.2017.03.019>.
 64. Mittal A, Raber AS, Schaefer UF, Weissmann S, Ebensen T, Schulze K, Guzmán CA, Lehr C-M, Hansen S. Non-invasive delivery of nanoparticles to hair follicles: a perspective for transcutaneous immunization. *Vaccines*. 2013;31:3442–51. <https://doi.org/10.1016/j.vaccine.2012.12.048>.
 65. Lademann J, Richter H, Schaefer U, Blume-Peytavi U. Hair follicles – a long-term reservoir for drug delivery. *Skin Pharmacol Physiol*. 2006;19:232–6. <https://doi.org/10.1159/000093119>.
 66. Gloor M. How do dermatological vehicles influence the horny layer? *Skin Pharmacol Physiol*. 2004;17:267–73. <https://doi.org/10.1159/000081111>.
 67. Schaller M, Laude J, Bodewaldt H, Hamm G, Korting HC. Toxicity and antimicrobial activity of a hydrocolloid dressing containing silver particles in an ex vivo model of cutaneous infection. *Skin Pharmacol Physiol*. 2004;17:31–6. <https://doi.org/10.1159/000074060>.
 68. Parhi R, Swain S. Transdermal evaporation drug delivery system: concept to commercial products. *Adv Pharm Bull*. 2018;8(4):535–50. <https://doi.org/10.15171/apb.2018.063>

69. Verma DD, Verma S, McElwee KJ, Freyschmidt-Paul P, Hoffman R, Fahr A. Treatment of alopecia areata in the DEBR model using cyclosporine – a lipid vesicles. *Eur J Dermatol.* 2004;14:332–8.
70. Warner RR, Stone KJ, Boissy YL. Hydration disrupts human stratum corneum ultrastructure. *J Invest Dermatol.* 2003;120:275–84. <https://doi.org/10.1046/j.1523-1747.2003.12046.x>.
71. Welin-Berger K, Neelissen JA, Bergenståhl B. The effect of rheological behaviour of a topical anaesthetic formulation on the release and permeation rates of the active compound. *Eur J Pharm Sci.* 2001;13:309–18. [https://doi.org/10.1016/S0928-0987\(01\)00118-X](https://doi.org/10.1016/S0928-0987(01)00118-X).
72. Fu Y, Kao WJ. Drug release kinetics and transport mechanisms of non-degradable and degradable polymeric delivery systems. *Expert Opin Drug Deliv.* 2010;7:429–44. <https://doi.org/10.1517/17425241003602259>.
73. Rastogi SK, Singh J. Lipid extraction and transport of hydrophilic solutes through porcine epidermis. *Int J Pharm.* 2001;225:75–82. [https://doi.org/10.1016/S0378-5173\(01\)00766-9](https://doi.org/10.1016/S0378-5173(01)00766-9).
74. Consonni D, Bertazzi PA. Health significance and statistical uncertainty. The value of P-value. *Med Lav.* 2017;108:327–31. <https://doi.org/10.23749/mdl.v108i5.6603>
75. López-García J, Lehocký M, Humpolíček P, Sáha P. HaCaT keratinocytes response on antimicrobial atelocollagen substrates: extent of cytotoxicity, cell viability and proliferation. *J Funct Biomater.* 2014;5:43–57. <https://doi.org/10.3390/jfb5020043>.
76. Place TL, Domann FE, Case AJ. Limitations of oxygen delivery to cells in culture: an underappreciated problem in basic and translational research. *Free Radic Biol Med.* 2017;113:311–22. <https://doi.org/10.1016/j.freeradbiomed.2017.10.003>.

Publisher's Note Springer Nature remains neutral with regard to jurisdictional claims in published maps and institutional affiliations.

Springer Nature or its licensor (e.g. a society or other partner) holds exclusive rights to this article under a publishing agreement with the author(s) or other rightsholder(s); author self-archiving of the accepted manuscript version of this article is solely governed by the terms of such publishing agreement and applicable law.